NASA Technical Memorandum 104466
ASME-91-GT-217

CFD Analysis of Jet Mixing in Low NO_x Flametube Combustors

M.V. Talpallikar and C.E. Smith
CFD Research Corporation
Huntsville, Alabama

M.C. Lai
Wayne State University
Detroit, Michigan

and

J.D. Holdeman
Lewis Research Center
Cleveland, Ohio

Prepared for the
36th International Gas Turbine and Aeroengine Congress and Exposition
sponsored by the American Society of Mechanical Engineers
Orlando, Florida, June 3-6, 1991

NASA

CFD ANALYSIS OF JET MIXING IN LOW NO_x FLAMETUBE COMBUSTORS

M. V. Talpallikar and C. E. Smith
CFD Research Corporation
Huntsville, AL 35805

M. C. Lai
Wayne State University
Detroit, MI 48202

J. D. Holdeman
NASA Lewis Research Center
Cleveland, OH 44135

ABSTRACT

The Rich-burn/Quick-mix/Lean-burn (RQL) combustor has been identified as a potential gas turbine combustor concept to reduce NO_x emissions in High Speed Civil Transport (HSCT) aircraft. To demonstrate reduced NO_x levels, cylindrical flametube versions of RQL combustors are being tested at NASA Lewis Research Center. A critical technology needed for the RQL combustor is a method of quickly mixing by-pass combustion air with rich-burn gases.

In this study, jet mixing in a cylindrical quick-mix section was numerically analyzed. The quick-mix configuration was five inches in diameter and employed twelve radial-inflow slots. The numerical analyses were performed with an advanced, validated 3-D Computational Fluid Dynamics (CFD) code named REFLEQS. Parametric variation of jet-to-mainstream momentum flux ratio (J) and slot aspect ratio was investigated. Both non-reacting and reacting analyses were performed.

Results showed mixing and NO_x emissions to be highly sensitive to J and slot aspect ratio. Lowest NO_x emissions occurred when the dilution jet penetrated to approximately mid-radius. The viability of using 3-D CFD analyses for optimizing jet mixing was demonstrated.

NOMENCLATURE

A	Pre-exponential Factor
D	Diameter of Quick-Mix Section
D_h	Hydraulic Diameter
EI	Emission Index
E/R	Activation Energy/Gas Constant
J	Jet-to-Mainstream Momentum Flux Ratio
m_i	Mass Flow in Each Cell i
m_j	Jet Mass Flow
m_∞	Mainstream Mass Flow
σ_T	Mass Weighted Standard Deviation of Temperature
n	Optimum Number of Slots
NO_x	Oxides of Nitrogen
T_{avg}	Mass-Weighted Average Temperature
T_i	Temperature in Each Cell i
u´	RMS of U Velocity
U	Averaged Axial Velocity
v´	RMS of V Velocity
V	Averaged Radial Velocity

INTRODUCTION

In order to meet the growing need for faster transportation, High-Speed Civil Transport (HSCT) aircraft and associated propulsion systems have been under study in recent years. One major concern that has surfaced concerning HSCT engines is their impact on deteriorating the earth's ozone layer. Using current technology, a fleet of HSCT aircraft would produce large amounts of oxides of nitrogen (NO_x) while cruising in the stratosphere. Such high levels of NO_x, through a series of well known reactions, would drastically reduce ozone levels. In order to reduce NO_x emissions, technology must be developed to design advanced, low emission combustors.

One combustor concept that has been identified as a leading candidate to reduce NO_x emissions is the Rich-burn/Quick-mix/Lean-burn (RQL) combustor. Originally conceived and developed for industrial combustors (Mosier and Pierce, 1980 and Pierce *et al.* , 1980), the RQL concept utilizes staged burning, as shown in Figure 1. Combustion is initiated in a fuel rich zone at equivalence ratios between 1.2 and 1.8, thereby reducing NO_x formation by depleting the available oxygen. Bypass combustion air is introduced in a quick-mix section and lean combustion occurs downstream at an overall equivalence ratio between 0.5 and 0.7. The quick-mix section usually has a smaller geometric cross-section area than the rich burn zone in order to prevent backflow and enhance mixing.

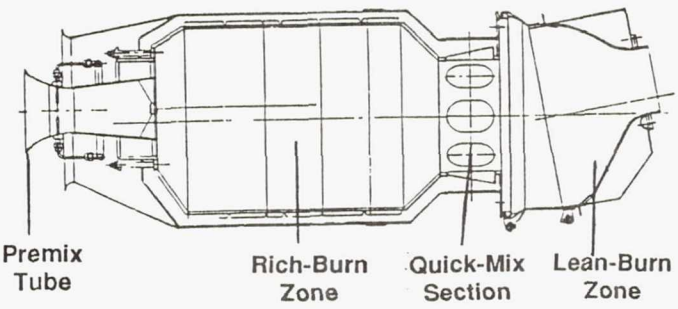

Fig. 1. Industrial Rich-burn/Quick-mix/ Lean-burn (RQL) Combustor (Pierce *et al.* , 1980)

Perhaps the single most important issue of the RQL concept is the design of the quick-mix section. For previous laboratory combustors,

Tacina (1990) has shown RQL NO_x levels to be higher than lean, premixed combustor NO_x levels. The higher NO_x emissions for RQL was attributed to stoichiometric burning in the quick-mix section, thus emphasizing the need for optimized rapid mix concepts. Indeed, Nguyen *et al.* (1989) have shown that if instantaneous mixing is assumed in the quick-mix section, low NO_x emission index can be obtained at HSCT cruise flight conditions. Hence, one challenge of the RQL concept is to identify quick-mix sections with rapid mixing.

This study sought to investigate the influence of jet-to-mainstream momentum flux ratio (J) and slot aspect ratio (SAR) on mixing effectiveness in a RQL flametube combustor to be tested at NASA Lewis Research Center (LeRC). Conventionally, dilution air in can combustors has been introduced through radial inflow holes. According to Holdeman's correlation (Holdeman *et al.*, 1987), optimum mixing occurs when the following expression is satisfied:

$$n = \pi \frac{\sqrt{2J}}{C} \tag{1}$$

where

n = optimum number of holes
C = experimentally derived constant ~2.5
J = jet-to-mainstream momentum flux ratio ($\rho_j V_j^2 / \rho_\infty V_\infty^2$).

Unfortunately, this correlation was developed for circular holed dilution jet mixing and jet mass flow-to-mainstream mass flow ratios (m_j/m_∞) of approximately 0.5. The RQL combustor requires m_j/m_∞ of 2.0, thus necessitating slots instead of holes around the can's perimeter. The design of slots for optimum mixing needs further investigation, and was the focus of this study.

CFD CODE

The approach in this study was to perform 3-D numerical computations on a cylindrical quick-mix section. The goal of the study was to provide improved understanding of slot injection and mixing. An advanced CFD code, REFLEQS, was used to perform the computations. REFLEQS was developed by CFD Research Corporation (Przekwas *et al.*, 1990 and Smith *et al.*, 1988) to analyze turbulent, reacting flows. The basic capabilities/methodologies in REFLEQS include:

1. solution of two and three-dimensional Navier-Stokes equations for incompressible and compressible flows;
2. cartesian, polar, and non-orthogonal body-fitted coordinates;
3. porosity-resistivity technique for flows with internal blockages;
4. fully implicit and strongly conservative formulation;
5. three differencing schemes: upwind, hybrid, and central differencing with damping terms;
6. standard (Launder and Spalding, 1974) and extended (Chen and Kim, 1987) k-ε turbulence models, the two-scale turbulence model of Kim and Chen (1988), and the low-Reynolds number k-ε model of Chien (1985);
7. instantaneous, one-step, and two-step combustion models;
8. modified form of Stone's Strongly Implicit Solver; and
9. pressure-based solution algorithms including SIMPLE and a variant of SIMPLEC.

REFLEQS has undergone a considerable amount of systematic quantitative validation for both incompressible and compressible flows. Over 30 validation cases have been performed to date, and good-to-excellent agreement between benchmark data and predictions has been shown (Smith *et al.*, 1989; Ratcliff and Smith, 1989; and Avva *et al.*, 1990). The good agreement gives confidence in the numerical results of this study.

HEAT RELEASE MODEL

After reviewing the time scales for heat release at cruise-type conditions in RQL mixers, it was determined reaction rates were much faster than mixing rates. Hence, the combustion process was considered mixing controlled, and instantaneous reaction rates for heat release were assumed.

When rich burn gases (composed of equilibrium concentration of CO, CO_2, H_2, H_2O and N_2) were mixed with air, they were assumed to react according to the equation:

$$0.0570\ CO + 0.0197\ CO_2 + 0.0383\ H_2 + 0.0680\ H_2O + 0.1371\ N_2$$
$$+ 0.1047\ O_2 + 0.3953\ N_2$$
$$\rightarrow 0.0767\ CO_2 + 0.1063\ H_2O + 0.7123\ N_2 + 0.0565\ O_2 \tag{2}$$

Accordingly, any CO concentration that remained in the mixer exit was the result of unmixedness.

NO_x MODEL

It was assumed that the NO_x reactions did not contribute to the overall heat release in the combustor, thus allowing the NO_x reactions to be "decoupled" from the heat release reactions. NO_x was calculated as a passive scalar after the computation of the reacting flowfield.

A simple Zeldovich reaction scheme was used to model the NO_x formation. According to the mechanism, *NO* formation can be described by:

$$N_2 + O \leftrightarrow NO + N \tag{3}$$

and

$$O_2 + N \leftrightarrow NO + O. \tag{4}$$

The first reaction is much slower than the second one and hence controls the rate of *NO* formation. If the concentration of *NO* is much smaller than the corresponding equilibrium value, the rate equation for *NO* can be written as:

$$\frac{d(NO)}{dt} = K\ [N_2]\ [O] \tag{5}$$

Approximating the concentrations of N_2 and O by the local equilibrium values, the rate equation is given by

$$\frac{d\ (NO)}{dt} = A\ e^{-\left(\frac{E}{RT}\right)} [N_2][O_2]^{\frac{1}{2}} \tag{6}$$

From Quan *et al.*, (1972), the rate constants were determined to be:

$$A = 5.74 \times 10^4 \frac{1}{sec} \sqrt{\frac{moles}{m^3}} \tag{7}$$

$$\frac{E}{R} = 6.7 \times 10^{11}\,^\circ K \tag{8}$$

The NO_x model was calibrated against the experimental results of Anderson (1975), who used a premixed, prevaporized laboratory combustor. The REFLEQS test case consisted of premixed propane and air reacting in a straight channel and instantaneous heat release. The rate constants had to be modified to give good agreement with Anderson's data. The final constants used in this study were:

$$A = 3.3 \times 10^4 \frac{1}{sec} \sqrt{\frac{moles}{m^3}} \tag{9}$$

$$\frac{E}{R} = 1.03 \times 10^{14}\,^\circ K \tag{10}$$

Figure 2 shows the computed results compared to Anderson's data of Emission Index (EI) as a function of adiabatic flame temperature.

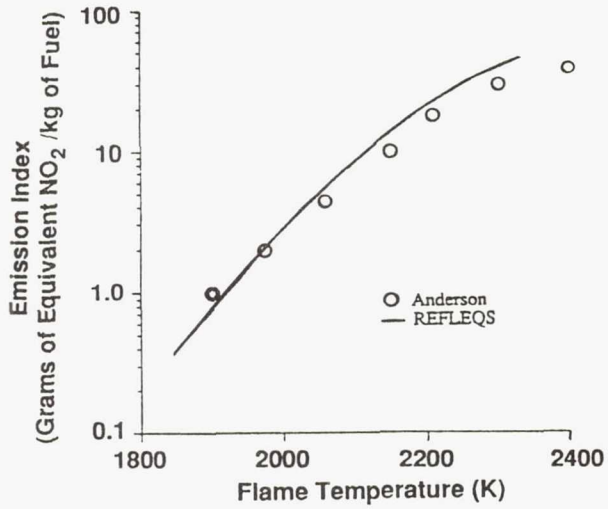

Fig. 2. Calibration of NO_x Model in REFLEQS

DETAILS OF NUMERICAL MODEL

A geometry compatible with the NASA LeRC flametube combustor was selected for analysis. The geometry, numerical grid, numerical details, boundary conditions, grid independence, and convergence criteria are discussed below.

Geometry

The geometry of the numerical model consisted of three components: an inlet pipe, converging section and a quick-mix section (see Figure 3). The inlet pipe was 0.152 m (6.0 in.) in diameter and 0.076 m (3.0 in.) in length. The inlet pipe converged into the quick-mix section which was 0.127 m (5.0 in.) in diameter (D). The length of the quick-mix section was 0.333 m (13.0 in.). In reality, the length of actual quick-mix section hardware is approximately 6 inches, but the computational domain is extended for better understanding of NO_x formation and to eliminate flowfield contamination by exit boundary conditions.

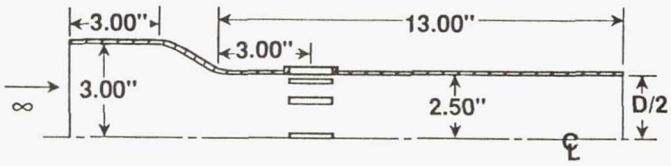

Fig. 3. Schematic of Quick-Mix Geometry

Twelve slots were located symmetrically around the perimeter of the quick-mix section. The axial location of the slot centerline was 0.076 m (3.0 in.) from the inlet of the quick-mix section. The baseline slots were rectangular in shape with an aspect ratio of four and aligned in the streamwise direction. Three variations in slot aspect ratio (SAR) were tested: 1, 4 and 16.

Due to geometric symmetry, only one slot was modeled with planes of symmetry set up halfway between adjacent slots. This allowed greater grid resolution and reduction of computer turnaround time. The rθ domain was reduced to a pie section with a central angle of thirty degrees.

Grid

A baseline grid of 9,216 cells (32x16x18 in x, r, θ directions) was selected and used for modeling the mixer. The grid is shown in Figure 4. Note that the origin of the coordinate system is located at the center of the slot. The axial grid spacing is dense near the slot, and gets coarser upstream and downstream of the slot. The grid in the radial direction was non-uniform with greater density near the combustor wall (power expansion of 1.2). The grid in the transverse direction was uniform in the slot, and slowly expanding away from the slot. The baseline slot was represented by a 6x6 mesh. As will be discussed in grid independence studies, this rather coarse grid is not grid-independent, but it does capture all of the relevant flow features. For comparative studies, it was felt sufficient.

Numerical Details

The numerical details of the calculations included:

1. Whole field solution of u-momentum, v-momentum, w-momentum, pressure correction, turbulent kinetic energy k, dissipation rate ε, total enthalpy, and mixture fraction;
2. Upwind Differencing for parametric studies of J and central differencing for parametric studies of SAR;
3. Variable Fluid Properties (*i.e.* temperature dependency of specific heat, laminar viscosity, *etc.*);
4. Adiabatic Walls;
5. Standard k-ε Model with wall functions;
6. Turbulent Prandtl number of 0.9;
7. Instantaneous heat-release model; and
8. Six active chemical species.

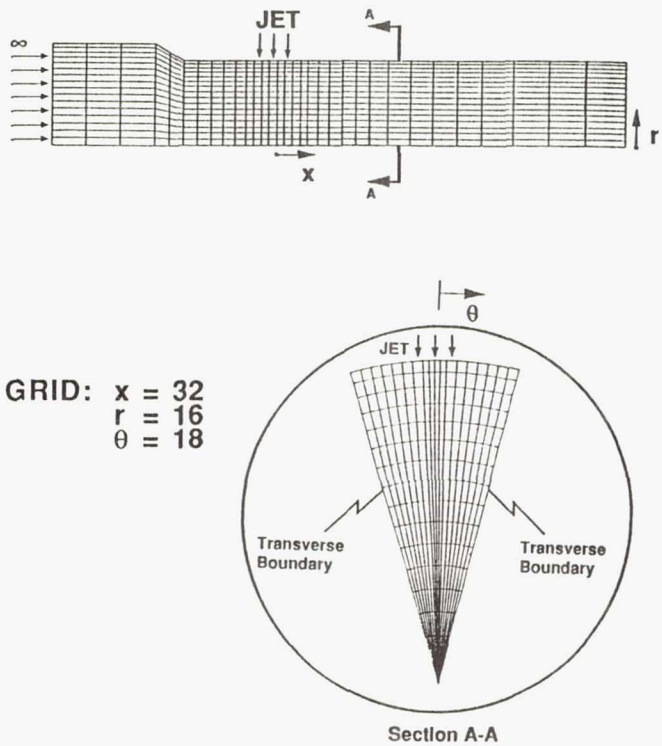

Fig. 4. Baseline Grid

Boundary Conditions

Mainstream Boundary. At the mainstream inlet boundary, propane and air are assumed to have completely reacted at an equivalence ratio (ϕ) of 1.6. The species and temperature of the reaction products were taken from the JANNAF-standard rocket code named One Dimensional Equilibrium (ODE) (Nickerson *et al.* , 1989).

Velocity and pressure were obtained from experimental test plans for the RQL flametube combustor. A uniform velocity profile was assumed with a turbulent intensity typical of primary zones in gas turbine combustors and a turbulent length scale corresponding to a turbulent viscosity 1000 times greater than laminar viscosity. The mainstream inlet conditions (at 6.0 in. diameter) were:

Axial velocity	= 35.5 m/s
Temperature	= 2221°K
Density	= 2.32 kg/m^3
Composition (mass fraction)	= 0.134 CO, 0.068 CO_2, 0.006 H_2, 0.096 H_2O, 0.696 N_2
Turbulent intensity (u′/U)	= 50%
Turbulent length scale (l_t/D_∞)	= 0.02

Since equilibrium NO_x levels are very low for ϕ of 1.6 (≈ 4 ppm), no NO_x was assumed in the mainstream inlet.

Jet Inlet. The composition at the dilution jet inlet was assumed to be air. A uniform velocity profile was assumed and turbulent properties were selected using the same logic as discussed for mainstream turbulence. The jet inlet flow conditions were:

Mass flux ratio (m_j/m_∞)	= 1.94
Jet temperature	= 811°K
Density	= 6.35 kg/m^3
Composition (mass fraction)	= 0.232 O_2, 0.768 N_2
Turbulent intensity (v′/V)	= 10%
Turbulent length scale (l_t/D_h)	= 0.13

The momentum flux ratio (J) was varied parametrically from 16 to 64 by variation of jet velocity from 120 m/s to 240 m/s. The jet velocity variation corresponded to liner pressure drops ($\Delta P/P$) of 3 to 12 percent. For each jet velocity, the slot flow area was modified to maintain constant jet flow.

Exit Boundary. The exit boundary condition was a zero gradient boundary condition.

Transverse Boundaries. The transverse boundaries were assumed to be symmetry planes. These boundaries were also tested for possible outflow by setting them to be periodic boundaries. No discernable difference was seen between cases with symmetric and periodic transverse boundaries.

Combustor Wall. The combustor wall was treated as a no-slip adiabatic wall (zero enthalpy gradient). Wall functions were used for the calculations of wall shear stress and near-wall turbulent quantities (k and ε).

Centerline. The computational boundary at the centerline was assumed to be a symmetry plane.

Grid Independence

Two different sizes of grids were run to test grid independence: 9,216 and 52,650 cells. The finer grid was obtained by increasing the grid density by ~75% in all three directions. Comparison of the two grids is shown in Figure 5.

Computational results from the two grids are presented in Figure 6 for a momentum flux ratio (J) of 32.0. The isotherms in an rx plane through the jet centerline are shown and compared. Qualitatively they exhibit similar features, although the jet penetrated a little further in the case of the fine grid. Isotherms are also shown for two axial planes: x/D = 0.0 and 2.0. The isotherms at x/D = 2.0 show slightly higher temperatures (~22°K) for the fine grid. Also, the cold region in the fine grid solution is located closer to the centerline, indicating greater penetration. However, overall the coarse grid solution is very similar to the fine grid solution.

Based on this grid-independence study, it appears the coarse grid captures the overall physics of the problem, and can be used to qualitatively compare quick-mix designs.

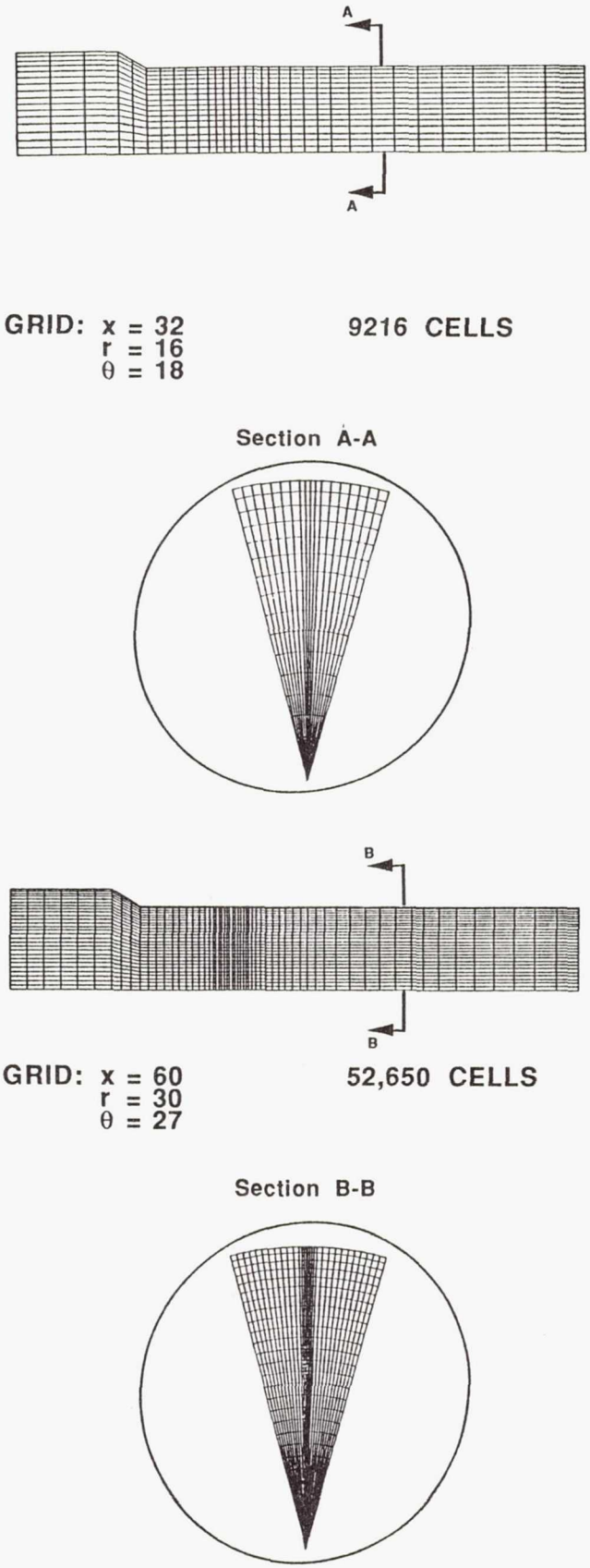

Fig. 5. Comparison of Coarse and Fine Grids

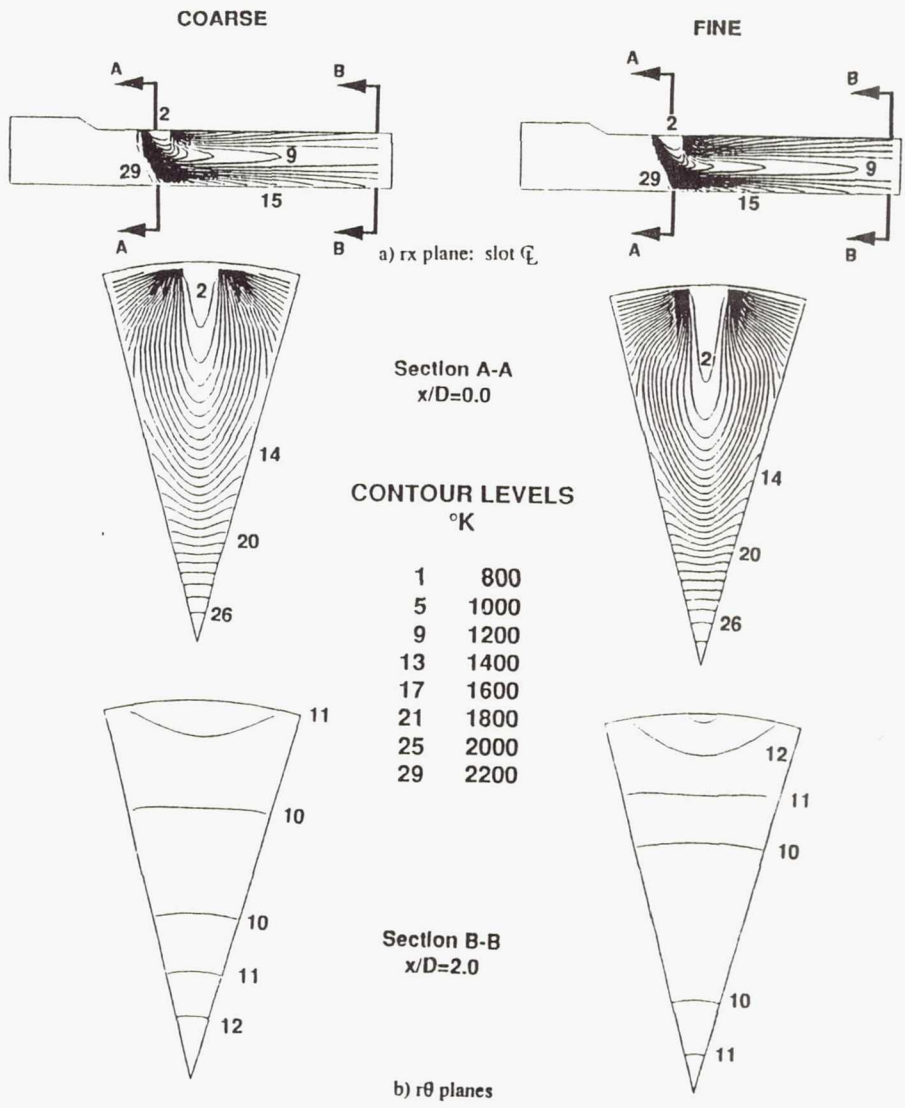

Fig. 6. Comparison of Isotherms for Coarse and Fine Grids: J=32

Convergence

The summations of all error residuals were reduced five orders of magnitude, and continuity was conserved in each axial plane. Typically, convergence required approximately 150 iterations as shown in the Figure 7. The relaxation on the velocity components (u and v only) was continuously varied during the run through a user specified input file. The repeated variation of relaxation allowed resolution of different scales of numerical error. This was found to speed up convergence by a factor of six compared to constant relaxation. Approximately 3 CPU hours were required on an Alliant FX/8 mini-supercomputer (operating on one computational element). Fine grid calculations took approximately 500 iterations and 40 CPU hours. For comparison, the ALLIANT computer speeds are ~20 times slower than a CRAY X-MP.

RESULTS

Parametric numerical tests were performed for jet-to-mainstream momentum flux ratios (J), for both non-reacting and reacting gases. Parametric variation of slot aspect ratio (SAR) was also studied. Discussion of the findings are reported below.

Variation of J: Non-Reacting Flow

Five jet-to-mainstream momentum flux ratios were parametrically tested: 16, 32, 40, 48, and 64. All other flow conditions were held constant, including mass flow ratio (jet-to-mainstream) at 1.94. To maintain a constant mass flow, the slot size was changed for each J. The slot aspect ratio was held constant at four, and was always centered at the same location. The same number of grid cells were used in all cases. However, since the slot size was changing, the grid density had to be slightly altered for each case. This variation is thought to have a minimal effect on the results discussed below.

Computed temperature contour maps are presented at x/D of 1.0, as shown in Figure 8. The radial location of the lowest temperatures indicates the penetration location of the cold jet. As expected, increased jet penetration can be seen for larger values of J. Best mixing seems to occur when the jet penetrates to approximately mid-radius. J of 32 and J of 40 appear to be optimum mixers. For comparison, the optimum J is 45.6 using Eq. (1).

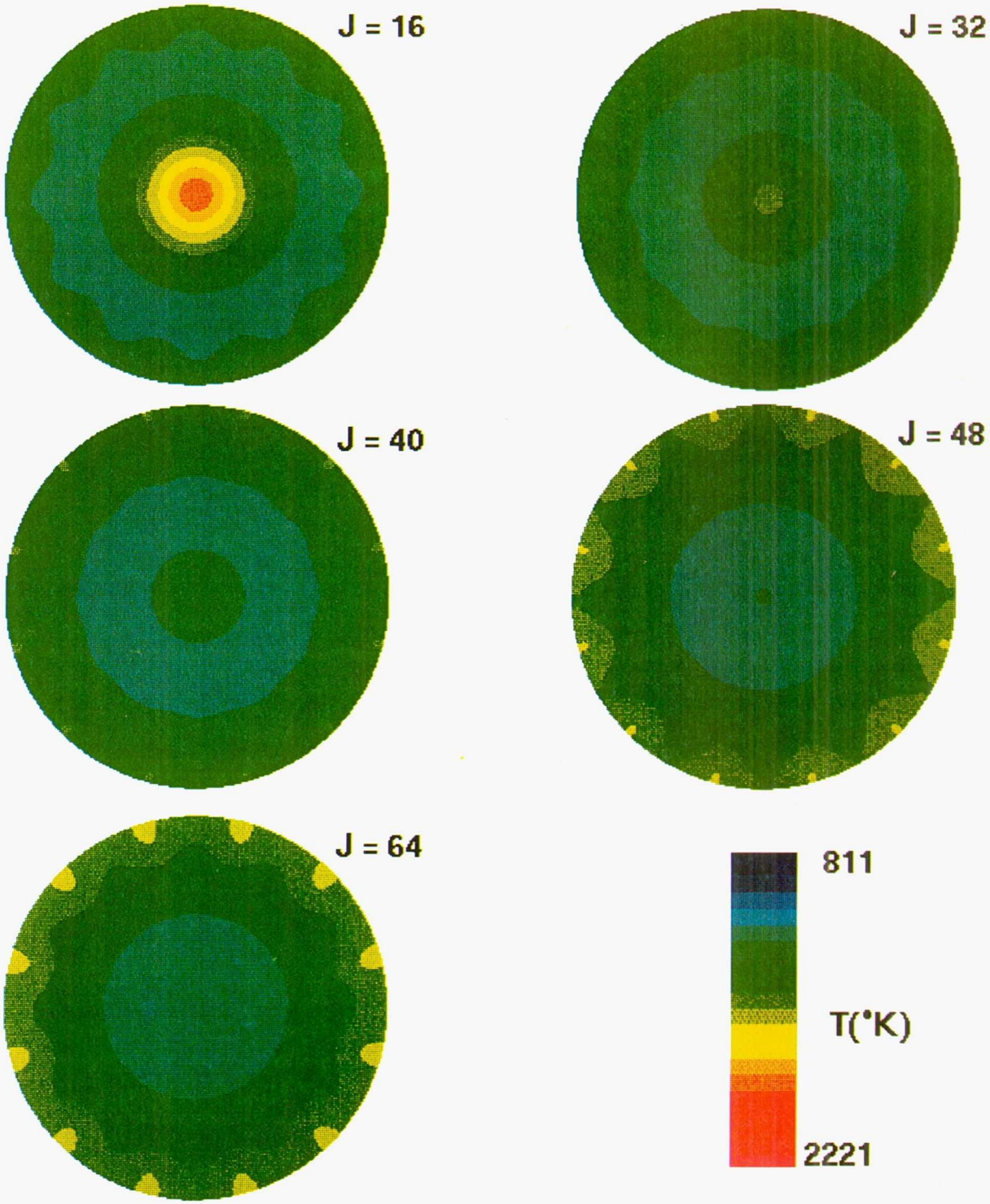

Fig 8. Temperature Contour Maps for Non-Reacting Conditions: x/D=1.0

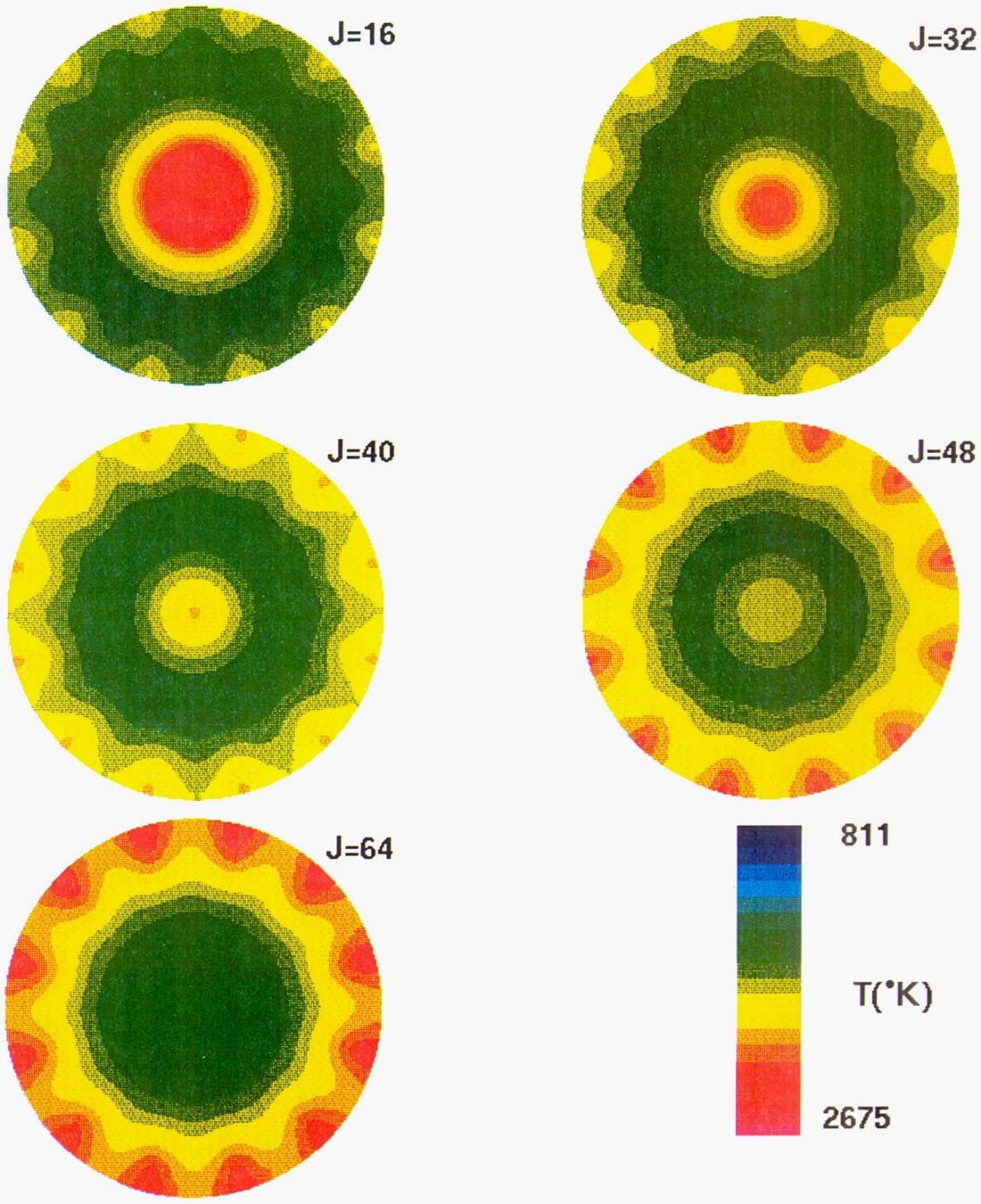

Fig 10. Temperature Contour Maps for Reacting Conditions: x/D=1.0

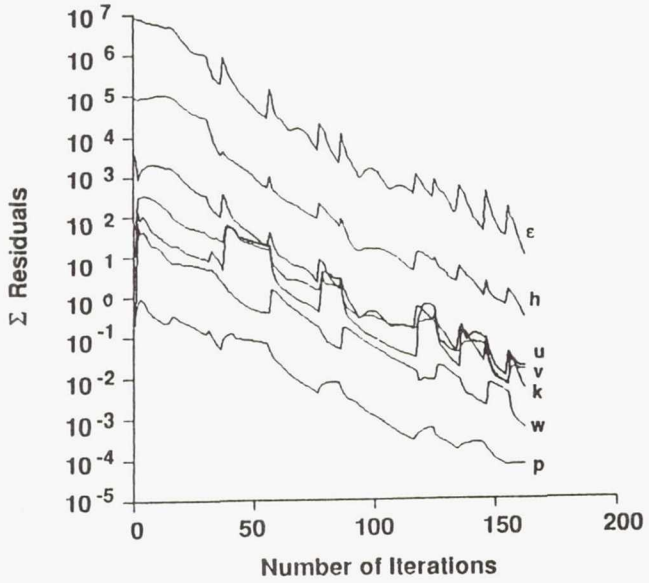

Fig. 7. Convergence History for a Typical Run

For a more quantitative comparison of mixing effectiveness, the mass-weighted standard deviation of temperature (σ_T) was calculated for each case. σ_T was defined as:

$$\sigma_T = \frac{\sqrt{\frac{\sum_i m_i (T_i - T_{avg})^2}{\sum_i m_i}}}{T_{avg}} \qquad (11)$$

In Figure 9, σ_T is presented versus J. It can be seen that J of 32 has the lowest σ_T at x/D = 2.0. Underpenetration is worse than over-penetration in terms of σ_T.

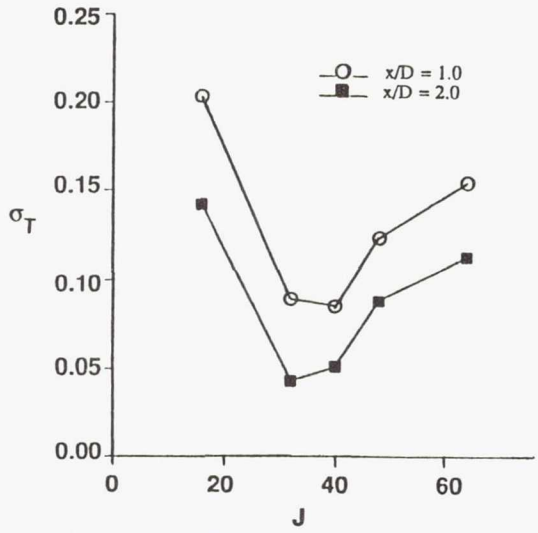

Fig. 9. Mixing Effectiveness: Non Reacting Flow

Variation of J: Reacting Flow

The same cases were analyzed as discussed above, except chemical reaction was turned on. Due to reaction, the overall mass-averaged exit temperature increased from 1301°K for non-reacting flows to 1790°K for reacting flows. Figure 10 shows temperature contour maps for the reacting cases one diameter downstream of the jet center. From this figure, it appears that J = 40 is the best mixer. This can be further elucidated by looking at the mixing effectiveness (σ_T) shown in Figure 11. Figure 11 shows J = 40 to be the best mixer at x/D = 1.0 and 2.0.

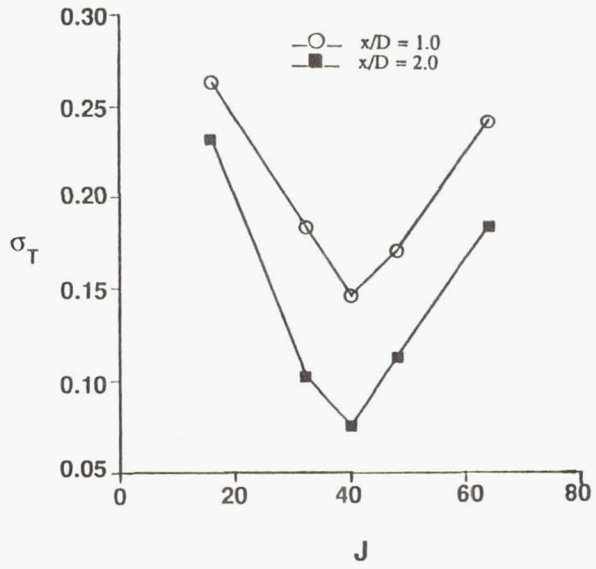

Fig. 11. Mixing Effectiveness: Reacting Flow

In addition to mixing effectiveness, another important criterion for evaluation of quick-mix sections is combustion efficiency. In particular, CO concentrations should be essentially eliminated from the combustor exit. The CO emission level in various axial planes downstream of the dilution jet is displayed in Figure 12. For all cases except J = 16, it can be seen that the CO species has been oxidized (to CO_2) by x/D = 0.25. For J = 16, unreacted CO remains in the flowfield even at x/D = 2.0. This is due to jet underpenetration, thus allowing rich burn gases (containing CO) on the centerline to pass through the quick-mix section without contact with dilution air.

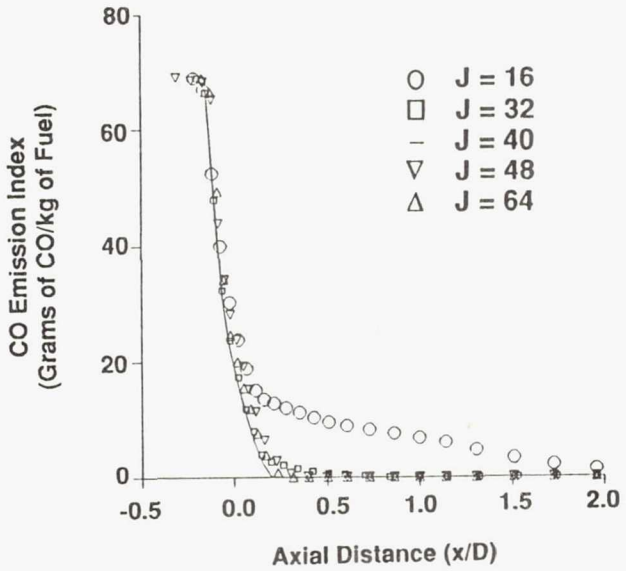

Fig. 12. Predicted CO Emissions

The NO_x results are presented in terms of Emission Index (EI) in Figure 13. For the optimum case (J_{opt}=40), EI is 2.9 at x/D = 2.0. Significant increase in EI is predicted as J is increased or decreased from the optimum value. For J greater than J_{opt}, jet overpenetration causes jet backflow on the centerline, resulting in higher NO_x emissions. For J less than J_{opt}, underpenetration of the jet results in reaction (and high temperatures) on the combustor centerline.

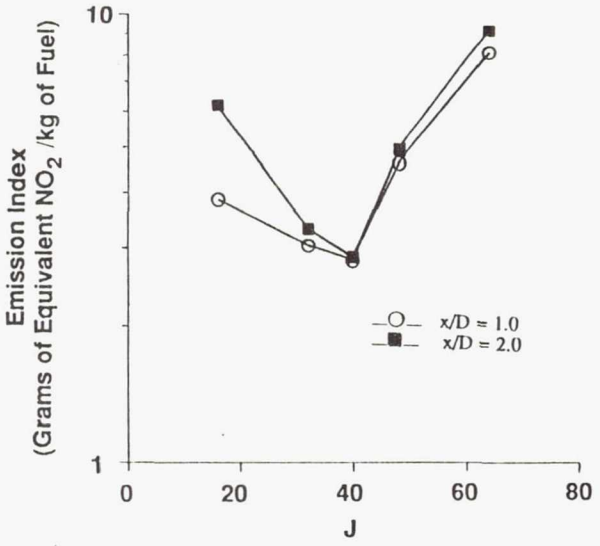

Fig. 13. Predicted NO_x Emission Index

Figure 14 shows NO_x concentrations convected out of each axial plane. Except for J = 16, all the cases show very little NO_x formation downstream of x/D = 1.0. This indicates that high temperature zones are no longer existent. For the J = 16 case, NO_x formation is increasing significantly downstream of x/D = 1.0, indicating high temperature and chemical reaction is still taking place.

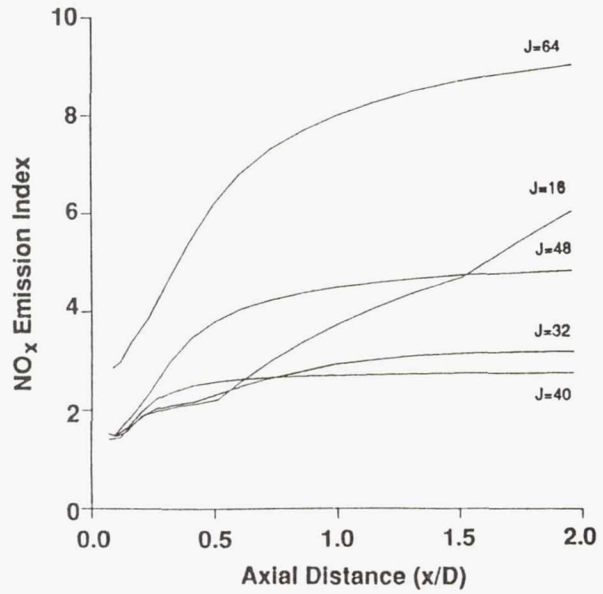

Fig. 14. History of NO_x Formation in Mixer

Variation of Slot Aspect Ratio

Three slot aspect ratios (SAR) were numerically analyzed: 1, 4 and 16. The long dimension was aligned in the mainstream flow direction. The numerical grid was slightly modified for each slot, and central differencing was employed for increased accuracy. The jet-to-mainstream momentum flux ratio and mass flow ratio was maintained constant at 32 and 1.94 respectively.

Isotherms in the rx plane through the jet centerline are shown in Figure 15. As SAR increased, jet penetration increased (as seen in Figure 15). This is due to reduced flow blockage as SAR is increased. Figure 16 shows the effect of SAR on NO_x emissions. For SAR of 1, predicted NO_x levels are less than those for SAR of 4, but chemical reaction and NO_x formation is still occurring at x/D of 1 due to jet underpenetration. This is evidenced by the steep slope of the NO_x curve at x/D of 1. A similar effect of delayed NO_x formation on the centerline caused by jet underpenetration was shown in Figure 14 for J of 16 and SAR of 4. Hence, the best SAR is 4, with jet overpenetration for SAR of 16 (and corresponding higher NO_x levels).

These results suggest the importance of SAR on NO_x emissions. As was shown earlier for J variation, the jet must penetrate to approximately mid-radius for optimum mixing, and hence lowest NO_x.

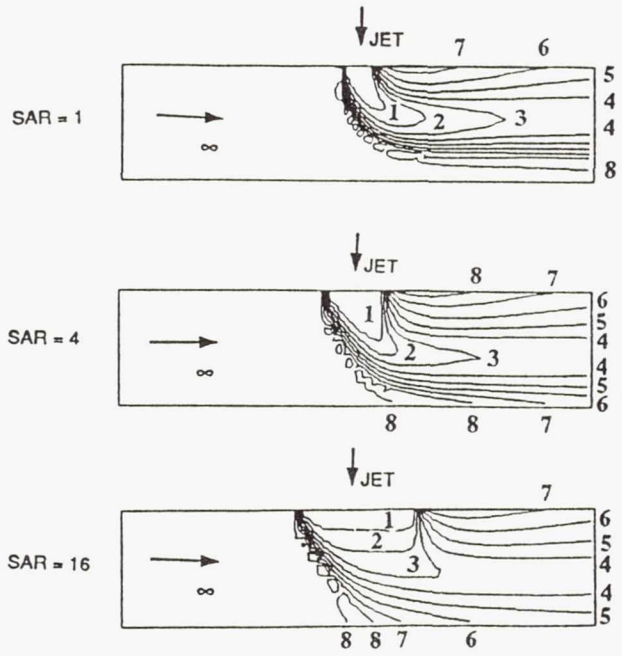

CONTOUR LEVELS

	°K
1	1000
2	1200
3	1400
4	1600
5	1800
6	2000
7	2200
8	2400

Fig. 15. Isotherms in rx Plane Through Jet Centerline: Effect of Slot Aspect Ratio (SAR)

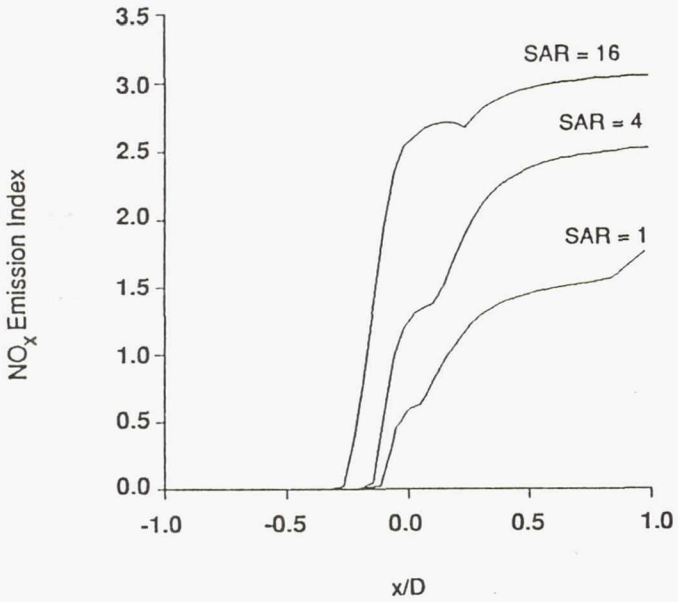

Fig. 16. Effect of Slot Aspect Ratio (SAR) on NO_x Emissions

CONCLUSIONS

The overall conclusions of this study were:

1. The viability of using 3-D CFD to model and screen quick-mix concepts of low emission combustors was successfully demonstrated.
2. A five-inch diameter quick-mix section compatible with the NASA LeRC Low Emission Combustor Program was numerically analyzed. The configuration consisted of twelve, radial-inflow slots uniformly distributed around the perimeter of the quick-mix section. Optimum mixing for non-reacting flow occurred for a jet-to-mainstream momentum flux ratio (J) between 32 and 40. For reacting flow, the NO_x emission index was shown to be **highly sensitive** to J, with the lowest value of 2.9 calculated for J of 40 (at x/D = 2.0).
3. The numerical results suggest that slot aspect ratio has a pronounced effect on jet penetration and mixing effectiveness. Conventional correlations for optimum mixing effectiveness for holes may not be applicable for slots.

ACKNOWLEDGEMENTS

The authors wish to thank NASA Lewis Research Center for funding this work under NASA Contract NAS3-25834. Our thanks also are extended to Drs. Laurence Keeton, H.Q. Yang, Andrzej Przekwas, Anantha Krishnan and Mr. Sami Habchi of CFD Research Corporation.

REFERENCES

Anderson, D., 1975, "Effect of Equivalence Ratios and Dwell Time on Exhaust Emissions from an Experimental Premixed Prevaporizing Burner," NASA TMX-71592.

Avva, R. K., Smith, C. E., and Singhal, A. K., 1990, "Comparative Study of High and Low Reynolds Number Versions of k- Models," AIAA-90-0246, 28*th Aerospace Sciences Meeting.*

Chen, Y. S., and Kim, S. W., 1987, "Computation of Turbulent Flows Using an Extended k-ε Turbulence Closure Model," NASA CR-179204.

Chien, K. Y., 1985, "Predictions of Channel and Boundary-Layer Flows with a Low-Reynolds-Turbulence Model," *AIAA Journal*, Vol. 23, No. 2.

Holdeman, J. D., Reynolds, R. and White, C., 1987, "A Numerical Study of the Effects of Curvature and Convergence on Dilution Jet Mixing," AIAA-87-1953, AIAA/SAE/ASME/ASEE 23*rd Joint Propulsion Conference.*

Kim, S. W., and Chen, C. P., 1988, "A Multiple Time Scale Turbulence Model Based on Variable Partitioning of Turbulent Kinetic Energy Spectrum," AIAA-88-1771.

Launder, B. E., and Spalding, D. B., 1974, "The Numerical Computation of Turbulent Flows," *Computer Methods in Applied Mechanics and Engineering*, Vol. 3, pp. 269-289.

Mosier, S. A., and Pierce, R. M., 1980, "Advanced Combustion Systems for Stationary Gas Turbine Engines," Vol. I, EPA Contract 68-02-2136.

Nguyen, H., Bittker, D., and Niedzwiecki, R., 1989, "Investigation of Low NO_x Staged Combustor Concept in High Speed Civil Transport Engines," AIAA-89-2942, AIAA/ASME/SAE/ASEE 25*th Joint Propulsion Conference.*

Nickerson, G. R., Coats, D. E., Dang, A. L., Dunn, S. S., and Kehtarnavaz, H., 1989, "Two-Dimensional Kinetics TDK Nozzle Performance Computer Program; Vol II: Programming Manual," NAS8-36863.

Pierce, R. M., Smith, C. E., and Hinton, B. S., 1980, "Advanced Combustion Systems for Stationary Gas Turbine Engines," Vol. III, EPA Contract 68-02-2136.

Przekwas, A. J., Habchi, S. D., Yang, H. Q., Avva, R. K., Talpallikar, M. V., and Krishnan, A., 1990, "REFLEQS-3D: A Computer Program for Turbulent Flows With and Without Chemical Reaction, Volume 1: User's Manual," CFD Research Corp., Huntsville, AL, CFDRC Report GR-89-4.

Quan, V., Marble, F. E., and Kliegel, J. R., 1972, "Nitric Oxide Formation in Turbulent Diffusion Flames," 14*th* Symposium on Combustion, pp. 851-860.

Ratcliff, M. L., and Smith, C. E., 1989, "REFLEQS-2D: A Computer Program for Turbulent Flow with and without Chemical Reaction; Volume 2: Validation Manual," CFD Research Corp., Huntsville, AL, CFDRC Report GR-88-4.

Smith, C. E., Ratcliff, M. L., Przekwas, A. J., Habchi, S. D., and Singhal, A. K., 1988, "Modeling of Turbulent Combustion in Liquid Rocket Engine Components," NASA MSFC Contract NAS8-37619, SBIR Phase I Final Report, CFDRC Report 4045/1.

Smith, C. E., Ratcliff, M. L., Przekwas, A. J., and Habchi, S. D., 1989, "Validation of an Advanced Turbulent Combustion Code: REFLEQS," 7*th* SSME CFD Workshop, NASA MSFC.

Tacina, R. R., 1990, "Low NO_x Potential Of Gas Turbine Engines," AIAA-90-0550, 28*th Aerospace Sciences Meeting.*

NASA
National Aeronautics and Space Administration

Report Documentation Page

1. Report No.	2. Government Accession No.	3. Recipient's Catalog No.
NASA TM-104466 ASME-91-GT-217		

4. Title and Subtitle

CFD Analysis of Jet Mixing in Low NO_x Flametube Combustors

5. Report Date

6. Performing Organization Code

7. Author(s)

M.V. Talpallikar, C.E. Smith, M.C. Lai, and J.D. Holdeman

8. Performing Organization Report No.

E-6313

10. Work Unit No.

537-02-21

9. Performing Organization Name and Address

National Aeronautics and Space Administration
Lewis Research Center
Cleveland, Ohio 44135-3191

11. Contract or Grant No.

13. Type of Report and Period Covered

Technical Memorandum

12. Sponsoring Agency Name and Address

National Aeronautics and Space Administration
Washington, D.C. 20546-0001

14. Sponsoring Agency Code

15. Supplementary Notes

Prepared for the 36th International Gas Turbine and Aeroengine Congress and Exposition sponsored by the American Society of Mechanical Engineers, Orlando, Florida June 3-6, 1991. M.V. Talpallikar and C.E. Smith, CFD Research Corporation, Huntsville, Alabama 35805 (work funded by NASA Contract NAS3-25834). M.C. Lai, Wayne State University, Detroit, Michigan 48202. J.D. Holdeman, NASA Lewis Research Center, (216) 433-5846.

16. Abstract

The Rich-burn/Quick-mix/Lean-burn (RQL) combustor has been identified as a potential gas turbine combustor concept to reduce NO_x emissions in High Speed Civil Transport (HSCT) aircraft. To demonstrate reduced NO_x levels, cylindrical flametube versions of RQL combustors are being tested at NASA Lewis Research Center. A critical technology needed for the RQL combustor is a method of quickly mixing by-pass combustion air with rich-burn gases. In this study, jet mixing in a cylindrical quick-mix section was numerically analyzed. The quick-mix configuration was five inches in diameter and employed twelve radial-inflow slots. The numerical analyses were performed with an advanced, validated 3-D Computational Fluid Dynamics (CFD) code named REFLEQS. Parametric variation of jet-to-mainstream momentum flux ratio (J) and slot aspect ratio was investigated. Both non-reacting and reacting analyses were performed. Results showed mixing and NO_x emissions to be highly sensitive to J and slot aspect ratio. Lowest NO_x emissions occurred when the dilution jet penetrated to approximately mid-radius. The viability of using 3-D CFD analyses for optimizing jet mixing was demonstrated.

17. Key Words (Suggested by Author(s))	18. Distribution Statement
Dilution; Jet mixing flow; Gas turbines; Combustion chamber; Can; Emissions	Unclassified - Unlimited Subject Category 07

19. Security Classif. (of the report)	20. Security Classif. (of this page)	21. No. of pages	22. Price*
Unclassified	Unclassified	14	A03

NASA FORM 1626 OCT 86

*For sale by the National Technical Information Service, Springfield, Virginia 22161